

Impact of stimulus fluctuations on perceptual decisions

Federico Fattorini

Università di Pisa

September 7, 2023



Introduction

Primacy vs recency

Perceptual decisions rely on the accumulation of sensory evidence.
Different models weight differently early and late stimulus evidence.
In particular:

- ▶ The *primacy* effect is the tendency to give more importance to early rather than late stimulus information.
- ▶ The *recency* effect is the tendency to give more weight to late rather than early stimulus information.



Introduction

Studied models

We will study the behaviours of 5 different models, in a binary classification task:

- ▶ DDMA: drift diffusion model with absorbing bounds.
- ▶ DDMR: drift diffusion model with reflecting bounds.
- ▶ PI: perfect integrator (drift diffusion with no bounds).
- ▶ DWM: double well model.
- ▶ Network model with spiking neurons.



Drift diffusion models

The evolution of the *decision variable* $x(t)$ is described by:

$$\tau \frac{dx}{dt} = S(t) + \sigma_I \xi_I(t)$$

where τ is the time scale of the process, $S(t)$ the *evidence* and the noise term (Gaussian) reflects the internal stochasticity of the process.

The evidence is characterised by a mean drift μ and by the stimulus fluctuation:

$$S(t) = \mu + \sigma_S \xi_S(t)$$

Finally:

$$\tau \frac{dx}{dt} = -\frac{d\phi(x)}{dx} + \sigma_S \xi_S(t) + \sigma_I \xi_I(t)$$

with $\phi(x) = -\mu x$



Drift diffusion models

Boundary conditions

DDMA, DDMR and PI are all drift diffusion models, but the shape of the potential is modified by decision bounds.

- ▶ The PI has no bounds.
- ▶ The DDMR implements *reflecting bounds*: when the decision variable reaches one of the two bounds, a limit is set to the accumulated evidence and x is reflected.
- ▶ The DDMA implements *absorbing bounds*: when the decision variable reaches one of the two bounds, it remains there for the rest of the trial.



Drift diffusion models

Simulations, $\mu = 0$

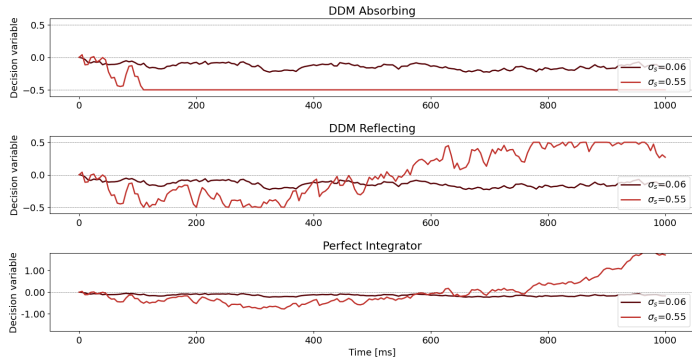


Figure: Simulation of the 3 models for 1 s with $\mu = 0$, $\tau = 200 \text{ ms}$, $\sigma_I = 0.1$ and two values of σ_S . Integration was performed with Euler method, with integration step $\Delta t = 5 \text{ ms}$.



Drift diffusion models

Simulations, $\mu = 0.15$

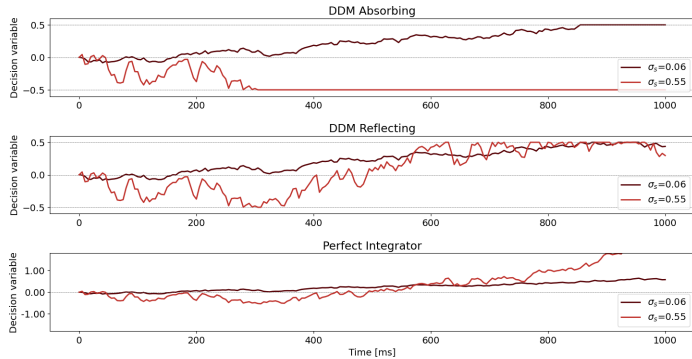


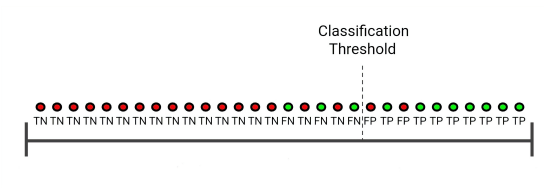
Figure: Simulation of the 3 models for 1 s with $\mu = 0.15$, $\tau = 200$ ms, $\sigma_I = 0.1$ and two values of σ_S . Integration was performed with Euler method, with integration step $\Delta t = 5$ ms.



Receiver Operating Characteristic (ROC)

A *binary classification* is a task that, given some data, assigns them to one of two mutually exclusive classes, the *positive* and the *negative* one.

Given a numerical predictor, a *classification threshold* allows to translate the numerical values in binary results, separating the positive by the negative class.



A *true positive* is an outcome where the model correctly predicts the positive class, a *false positive* is an outcome where the model incorrectly predicts the positive class.



Receiver Operating Characteristic (ROC)

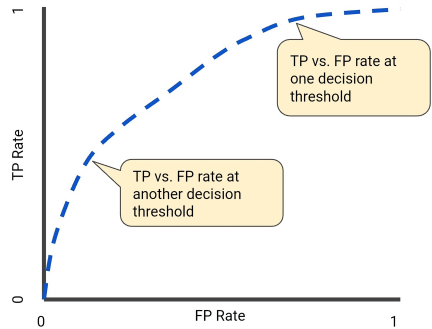
The *True Positive Rate* is defined as:

$$\frac{TP}{TP + FN}$$

The *False Positive Rate* is defined as:

$$\frac{FP}{FP + TN}$$

An ROC curve plots TPR vs FPR at different classification thresholds.



Psychophysical Kernel

The impact of the stimulus fluctuations on the final decisions during the course of the task is measured by the *Psychophysical Kernel* (PK).

Computation of PK

- ▶ For each trial i we consider the stimulus fluctuations for each time $s_i(t) = \sigma_S \xi_i(t)$ and we store the sign of the decision variable at the end of the trial, which represents the final choice.
- ▶ For each time t , we consider as predictions the fluctuations $s_i(t)$, and as two classes the final choices .
- ▶ Varying the classification thresholds in the range of the fluctuations, we build a ROC curve for each time t .
- ▶ The PK is defined as the temporal evolution of the area under the ROC curve (AUROC).



Drift diffusion models

Psychophysical Kernel for PI model

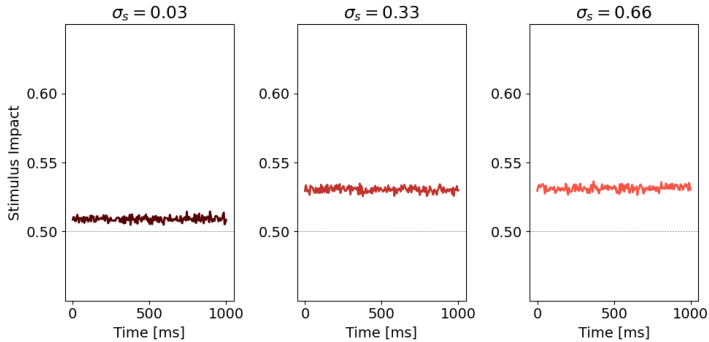


Figure: PK for PI model, for 3 different σ_S . 100000 trials were simulated with different realisations of noise. Parameters and integration method are the same above.



Drift diffusion models

Psychophysical Kernel for DDMR model

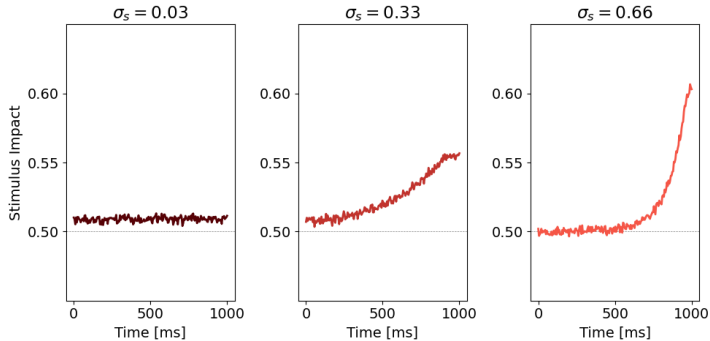


Figure: PK for DDMR model, for 3 different σ_S . 100000 trials were simulated with different realisations of noise. Parameters and integration method are the same above.



Drift diffusion models

Psychophysical Kernel for DDMA model

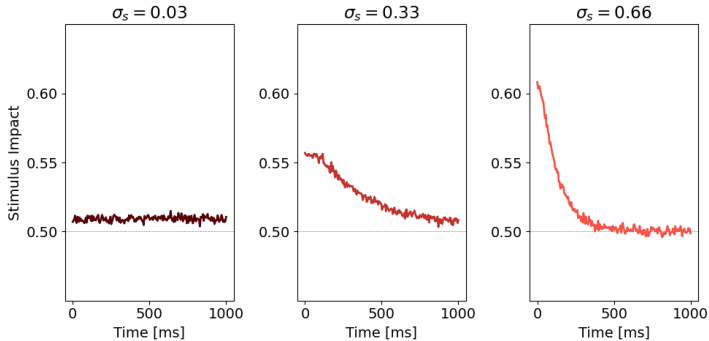


Figure: PK for DDMA model, for 3 different σ_s . 100000 trials were simulated with different realisations of noise. Parameters and integration method are the same above.



Drift diffusion models

Observations

- ▶ For small σ_S , the decision variable does not reach the bounds: there is no difference among the models.
- ▶ The Perfect Integrator model considers the stimulus fluctuations uniformly across time.
- ▶ The DDMR model shows a recency effect for sufficiently large fluctuations. Once the decision variable bounces on the decision bounds, early fluctuations are forgot.
- ▶ The DDMA model shows a primacy effect for sufficiently large fluctuations. Once the decision variable touches the decision bounds, the choice is made. Therefore, later fluctuations have lower weight in the decision process.



Double well model

The evolution of the decision variable $x(t)$ is described by:

$$\tau \frac{dx}{dt} = -\frac{d\phi(x)}{dx} + \sigma_S \xi_S(t) + \sigma_I \xi_I(t)$$

with $\phi(x) = -\mu x - \alpha x^2 + x^4$.

The terms of the potential describe:

- ▶ the impact of the net stimulus evidence μ , which tilts the potential toward the right choice;
- ▶ the height of the barrier between the two attractors, proportional to α^2 , defining the categorization dynamics;
- ▶ the limits of evidence accumulations, represented by the two possible minima.



Double well model

Simulations, $\mu = 0$

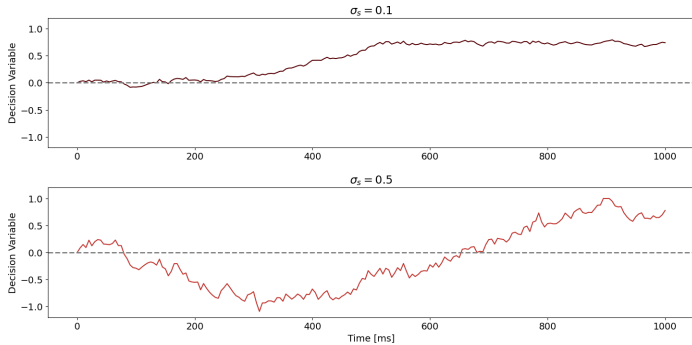


Figure: Simulation of the DWM model for 1 s with $\mu = 0$, $\tau = 200 \text{ ms}$, $\sigma_I = 0.1$, $\alpha = 1$ and two values of σ_S . Integration was performed with Euler method, with integration step $\Delta t = 5 \text{ ms}$.



Double well model

Psychophysical Kernel for different σ_S

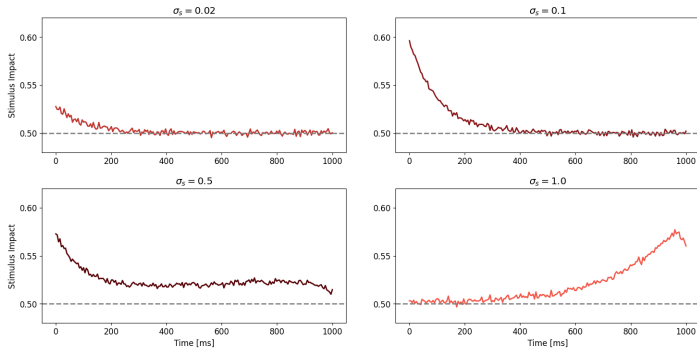


Figure: PK for DDMR model, for 4 different σ_S . 100000 trials were simulated with different realisations of noise. Parameters and integration method are the same above.



Double well model

Psychophysical Kernel for different T

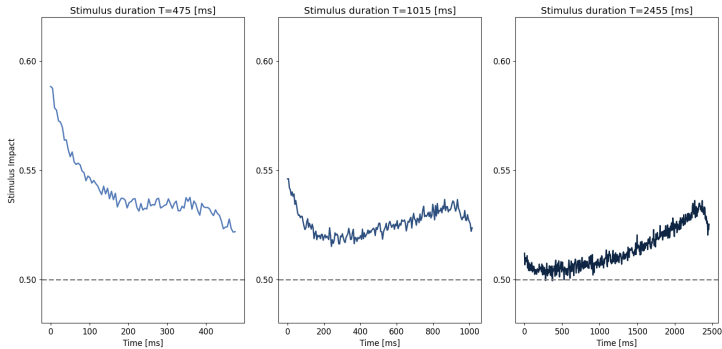


Figure: PK for DDMR model, for 3 different stimulus durations. 100000 trials were simulated with different realisations of noise. Parameters and integration method are the same above, $\sigma_S = 0.58$.



Double well model

Observations

- ▶ For small σ_S , categorisation dynamics dominates: the fluctuations cannot move the system from the chosen attractor. The system shows primacy effect, since early fluctuations influence the final choice.
- ▶ For large σ_S , only the late fluctuations matter in the final choice. The system shows recency.
- ▶ For intermediate σ_S the system is in the *flexible categorisation* regime. There is a balance between the internal categorisation dynamics, and the ability of the fluctuations to overcome the attraction of the potential.
- ▶ Flexible categorisation could be obtained varying the stimulus duration: the rate of transitions between the attractors is constant, but the probability increases with stimulus duration.



Accuracy for the DWM model

Psychometric function

The *psychometric function* $P(\mu, \sigma_S)$ shows the proportion of correct choices of the model as a function of the mean stimulus evidence μ and of the intensity of the stimulus fluctuations σ_S .

Mathematically:

$$P = P_0(1 - p_E) + (1 - P_0)p_C$$

where:

- ▶ P_0 is the probability of first visiting the correct attractor.
- ▶ p_C is the *correcting* transition probability, i.e., the probability of jumping into the right attractor, given that the first visited was the incorrect one.
- ▶ p_E is the *error-generating* transition probability, i.e., the probability of jumping into the wrong attractor, given that the first visited was correct.



Accuracy for the DWM model

Visiting probability

Assuming negligible the time spent in the unstable region, the probability of visiting the right attractor is:

$$P_0 = \frac{\int_{x_E}^{x_0} \exp\left(\frac{2\phi(x)}{\sigma_I^2 + \sigma_S^2}\right) dx}{\int_{x_E}^{x_C} \exp\left(\frac{2\phi(x)}{\sigma_I^2 + \sigma_S^2}\right) dx}$$

where x_C and x_E are the x values of the correct and incorrect attractor, and $x_0 = 0$ is the initial condition.

Neglecting the x^4 term:

$$P_0 = \frac{\operatorname{erf}\left(\frac{\sqrt{2\alpha}}{\sigma}\left(x_0 + \frac{\mu}{2\alpha}\right)\right) - \operatorname{erf}\left(\frac{\sqrt{2\alpha}}{\sigma}\left(x_E + \frac{\mu}{2\alpha}\right)\right)}{\operatorname{erf}\left(\frac{\sqrt{2\alpha}}{\sigma}\left(x_E + \frac{\mu}{2\alpha}\right)\right) - \operatorname{erf}\left(\frac{\sqrt{2\alpha}}{\sigma}\left(x_C + \frac{\mu}{2\alpha}\right)\right)}$$



Accuracy for the DWM model

Transition rates

By the use of the Arrhenius formula for the mean first-passage time in a double well potential, the correcting transition rate is:

$$k_C = \frac{\sqrt{|\phi''(x_E)\phi''(x_U)|}}{2\pi} \exp\left(-\frac{2(\phi(x_U) - \phi(x_E))}{\sigma_I^2 + \sigma_S^2}\right)$$

while the error transition rate is:

$$k_E = \frac{\sqrt{|\phi''(x_C)\phi''(x_U)|}}{2\pi} \exp\left(-\frac{2(\phi(x_U) - \phi(x_E))}{\sigma_I^2 + \sigma_S^2}\right)$$

where x_U is the unstable state.



Accuracy for the DWM model

Transition probabilities

Considering the model as a two states model, i.e., as a Random Telegraph, with transition rates k_C and k_E , the correcting and error-generating transition probabilities during a trial of duration T are:

$$p_C(T) = P_\infty(1 - \exp(-kT))$$

$$p_E(T) = (1 - P_\infty)(1 - \exp(-kT))$$

where $k = k_c + k_E$ and $P_\infty = \frac{k_c}{k_c + k_E}$ is the probability of the stationary state being the correct one.



Accuracy for the DWM model

Transition and first visit probabilities: analytical plots

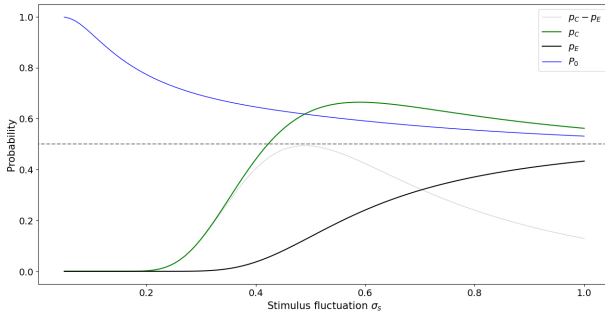


Figure: Analytical functions of correcting and error-generating transition probabilities, with their difference. First visit probability is also plotted.
 $\mu = 0.15$, $\sigma_I = 0$, $T = 2000$ ms, $\alpha = 1$.



Accuracy for the DWM model

Psychometric function

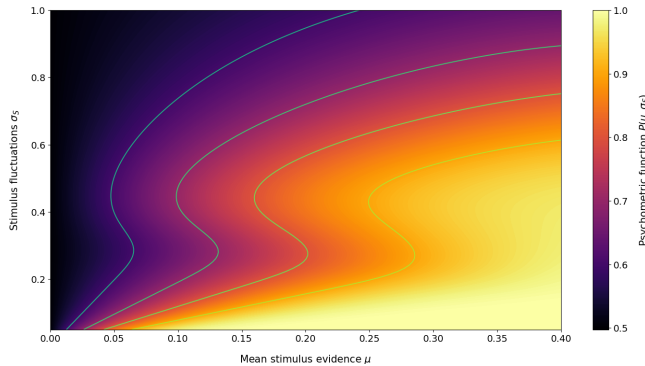


Figure: Contour plot of the psychometric function, with level curves.
 $T = 2000 \text{ ms}$, $\sigma_I = 0$, $\alpha = 1$.



Accuracy for the DWM model

Comparison between theoretical and simulated data

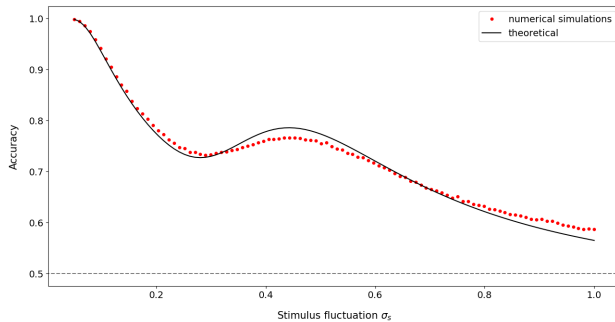


Figure: Analytical plot of $P(\sigma_s)$, and simulated values, for $\mu = 0.15$. For each value of σ_s , 100000 trials were simulated: accuracy is the fraction of correct choice among the trials. $T = 2000$ ms, $\sigma_I = 0$ $\alpha = 1$.



Accuracy for the DWM model

Observations

- ▶ For $\sigma_S \simeq 0$, the model is deterministic and $P=1$.
- ▶ For small σ_S , fluctuations are not large enough to generate transitions ($p_E \simeq p_C \simeq 0$) and accuracy is determined by P_0 .
- ▶ Because of the asymmetry of the potential $p_C > p_E$; in particular, when $p_C - p_E$ is maximum, the system is in the flexible categorisation regime because fluctuations are mainly correcting.
- ▶ For large σ_S , error transitions become likely as well, leading to a decrease of P .



Accuracy for the drift diffusion model

Simulated data

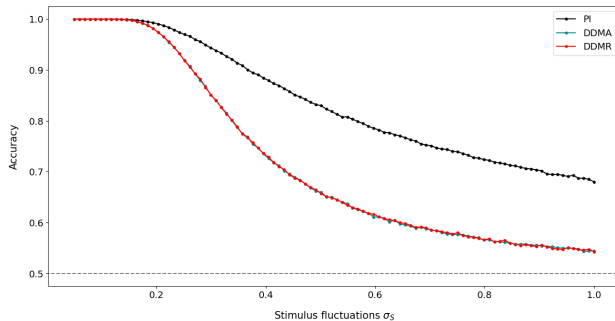


Figure: Simulated plots of $P(\sigma_S)$ for the models PI, DDMR and DDMA, with $\mu = 0.15$. For each value of σ_S , 100000 trials were simulated: accuracy is the fraction of correct choice among the trials. $T = 2000\text{ ms}$, $\sigma_I = 0$.



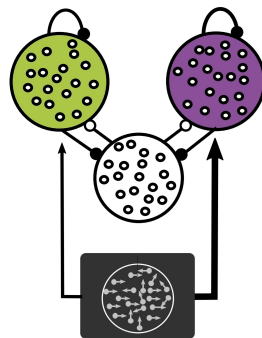
Network model

Structure

The network is composed by 4 populations of leaky integrate-and-fire neurons, with:

- ▶ Two populations of $N_E = 1000$ excitatory neurons, selective to the evidence supporting one of the two possible choices.
- ▶ A non-selective inhibitory population of $N_I = 500$ neurons.
- ▶ An external population of $N_{ext} = 1000$ neurons, represented with independent stochastic inputs.

The one of the 2 excitatory populations with the highest firing rate indicates the choice made by the network.



Network model

Equations for the membrane potential

The evolution for the membrane potential of the i th neuron in population X is given by:

$$\tau_m^E \frac{dV_i^A}{dt} = -(V_i^A - E_I) + I_i^{AA} - I_i^{AI} + \frac{I_i^{A_{ext}}}{g_L^E}$$

$$\tau_m^E \frac{dV_i^B}{dt} = -(V_i^B - E_I) + I_i^{BB} - I_i^{BI} + \frac{I_i^{B_{ext}}}{g_L^E}$$

$$\tau_m^I \frac{dV_i^I}{dt} = -(V_i^I - E_I) + I_i^{IA} - I_i^{IB} + \frac{I_i^{I_{ext}}}{g_L^I}$$

where I^{XY} are synaptic input voltages from neurons in population Y to neurons in population X , while $I^{X_{ext}}$ are the external synaptic inputs.



Network model

Synapses

The connectivity among the populations is random and sparse, with each neuron from population X receiving on average C_{XY} synapses from population Y .

The synaptic inputs take the form (sums over all the PSPs):

$$I_i^{XY} = \sum_j J_{ij}^{XY} g_{ij}^{XY}$$

choosing $J_{ij}^{AA} = J_{ij}^{BB} = J_{EE}$, $J_{ij}^{IA} = J_{ij}^{IB} = J_{IE}$ and $J_{ij}^{AI} = J_{ij}^{BI} = J_{EI}$



Network model

Synapses

If the presynaptic neuron j fires a spike at time t_k^{XY} , g_{ij}^{XY} is incremented by one at $t_k^{XY} + \delta_k^Y$, otherwise the dynamics of the synapses are described by:

$$\tau_s^Y \frac{dg_{ij}^{XY}}{dt} = -g_{ij}^{XY}$$

External synapses have instantaneous dynamics:

$$I_i^{ext} = \sum_j J_{ij}^{ext} \sum_k \delta(t - t_{k,j}^{X_{ext}})$$

A spike is emitted whenever the voltage of a cell crosses a threshold Θ , after which it is reset to potential E_r .



Network model

Stimulus

The stimulus inputs onto each of the excitatory populations are given by:

$$I_{stim}^A(t) = I_0(1 + \mu) + \sigma_S z^A(t)$$

$$I_{stim}^B(t) = I_0(1 - \mu) + \sigma_S z^B(t)$$

where μ parametrizes the mean difference of the two stimulus, capturing the evidence in favor of one of the 2 populations. $z^A(t)$ and $z^B(t)$ are independent realisations of an Ornstein-Uhlenbeck process:

$$\tau_{stim} \frac{dz}{dt} = -z + \sqrt{2\tau_{stim}} \xi(t)$$

In the simulations, stimulus presentation was preceded by a 500 ms interval to prevent transient effects due to initial conditions.



Network model

Model parameters: connectivity and neuron model

$J_{EE} = 0.16 \text{ mV}$	Weight of excitatory to excitatory connections
$J_{IE} = 0.08 \text{ mV}$	Weight of excitatory to inhibitory connections
$J_{EI} = -4 \text{ mV}$	Weight of inhibitory to excitatory connections
$C_{EE} = 100$	Average number of synapsis from excitatory to excitatory
$C_{IE} = 50$	Average number of synapsis from excitatory to inhibitory
$C_{EI} = 50$	Average number of synapsis from inhibitory to excitatory
$\tau_m^E = 20 \text{ ms}$	Membrane time constant of excitatory neurons
$\tau_m^I = 10 \text{ ms}$	Membrane time constant of inhibitory neurons
$g_L^E = 12.5 \text{ nS}$	Leak conductance of excitatory neurons
$g_L^I = 25 \text{ nS}$	Leak conductance of inhibitory neurons
$E_I = -70 \text{ mV}$	Resting potential
$\Theta = -50 \text{ mV}$	Spiking threshold
$E_r = -60 \text{ mV}$	Reset potential



Network model

Model parameters: synapses model, external Poisson inputs and stimulus

$\tau_S^E = 12.5 \text{ ms}$	Time constant of excitatory synapses
$\tau_S^I = 1 \text{ ms}$	Time constant of inhibitory synapses
$\delta_E = 5 \text{ ms}$	Mean delay for excitatory synapses (distribution: $U(0, 10)$)
$\delta_I = 1 \text{ ms}$	Mean delay for inhibitory synapses (distribution: $U(0, 2)$)

$J_{\text{ext}} = 0.2 \text{ mV}$	Weight of external inputs
$\nu_{\text{ext}}^E = 5000 \text{ Hz}$	Firing rate of external Poisson inputs to excit. neurons
$\nu_{\text{ext}}^I = 9000 \text{ Hz}$	Firing rate of external Poisson inputs to inhib. neurons

$I_0 = 25 \text{ pA}$	Mean input for zero-coherence stimulus
$\mu = 0.015$	Additional input for non-zero coherence stimulus
σ_S	Amplitude of noise fluctuations of the stimulus
$\tau_{\text{stim}} = 20 \text{ ms}$	Time constant of the Ornstein-Uhlenbeck process



Network model

Simulations for $\sigma_S = 2 \text{ pA}$ and $\mu = 0.015$

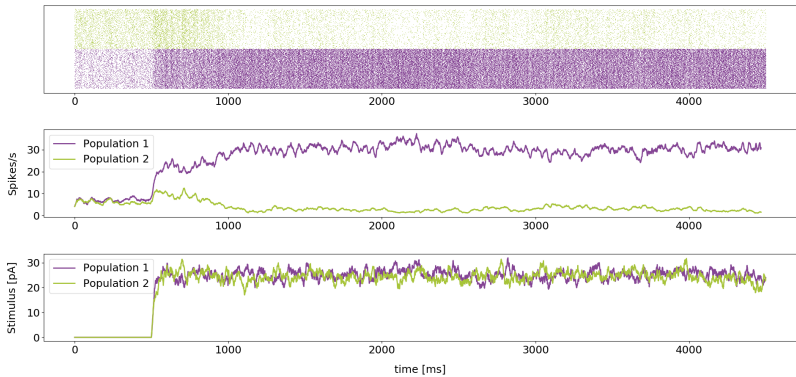


Figure: Raster plots, firing rates (smoothed on a window of 30 ms) and stimuli for the excitatory populations.



Network model

Psychophysical Kernel for $\sigma_S = 2 \text{ pA}$ and $\mu = 0.015$

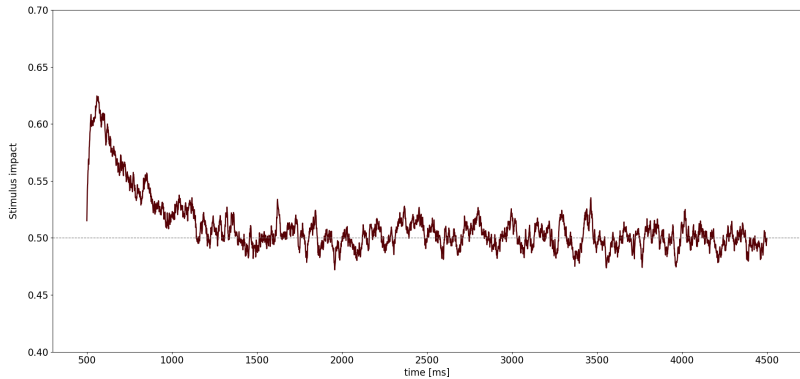


Figure: PK computed on 5000 different realisations of the stimulus and of the connectivities.



Network model

Simulations for $\sigma_S = 4.5 \text{ pA}$ and $\mu = 0.015$

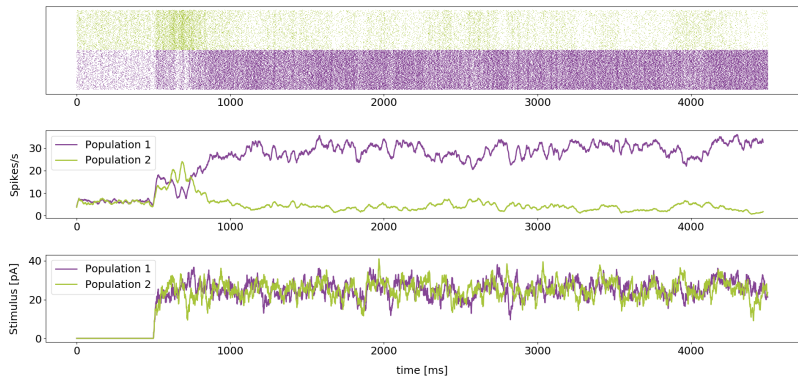


Figure: Raster plots, firing rates (smoothed on a window of 30 ms) and stimuli for the excitatory populations.



Network model

Psychophysical Kernel for $\sigma_S = 4.5 \text{ pA}$ and $\mu = 0.015$

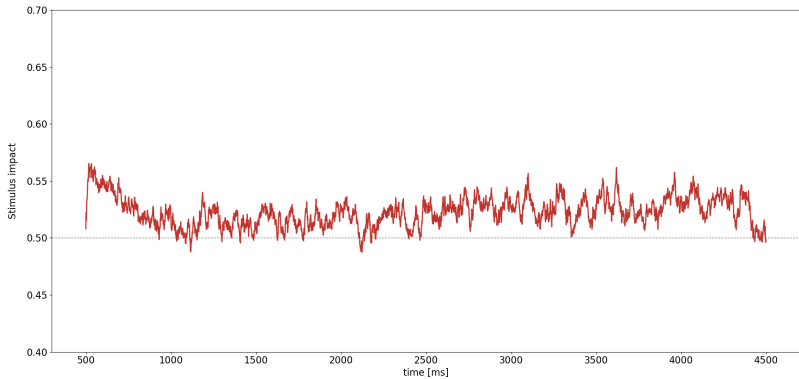


Figure: PK computed on 5000 different realisations of the stimulus and of the connectivities.



Network model

Simulations for $\sigma_S = 9 \text{ pA}$ and $\mu = 0.015$

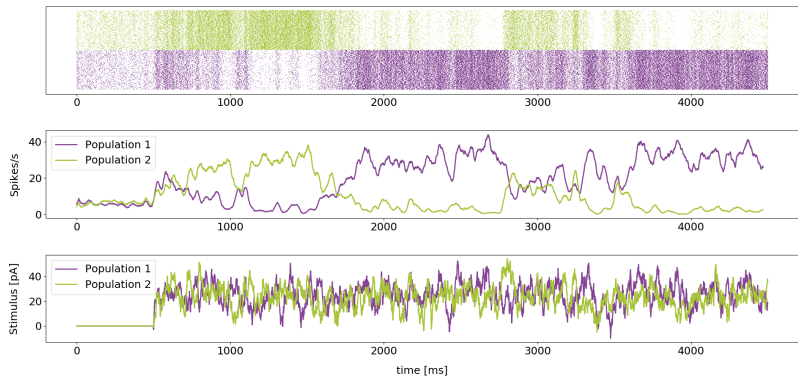


Figure: Raster plots, firing rates (smoothed on a window of 30 ms) and stimuli for the excitatory populations.



Network model

Psychophysical Kernel for $\sigma_S = 9 \text{ pA}$ and $\mu = 0.015$

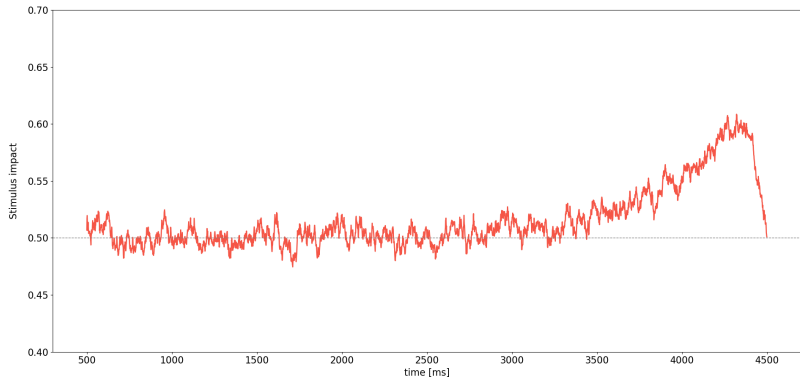


Figure: PK computed on 5000 different realisations of the stimulus and of the connectivities.



Network model

Psychophysical Kernel for different stimulus durations

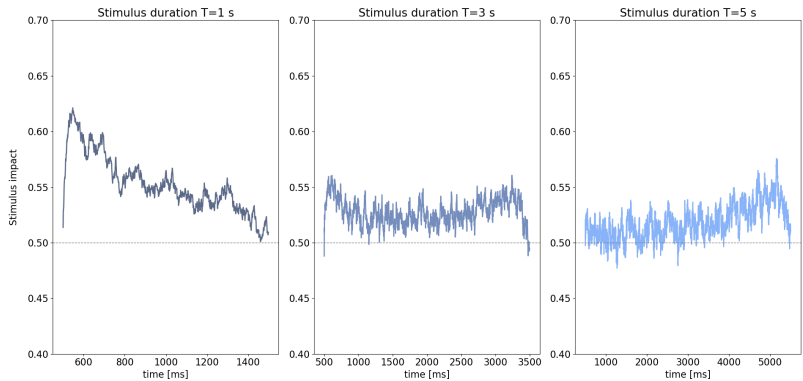


Figure: PK computed on 5000 different realisations of the stimulus and of the connectivities. σ_S was fixed at 5 pA.



Bibliography

- [1] C. W. Gardiner and C. W. Gardiner. *Stochastic methods: a handbook for the natural and social sciences*. 4th ed. Springer series in synergetics. Berlin: Springer, 2009. ISBN: 9783540707127.
- [2] H.A. Kramers. "Brownian motion in a field of force and the diffusion model of chemical reactions". en. In: *Physica* 7.4 (Apr. 1940), pp. 284–304. ISSN: 00318914. DOI: 10.1016/S0031-8914(40)90098-2. URL: <https://linkinghub.elsevier.com/retrieve/pii/S0031891440900982>.
- [3] Genís Prat-Ortega et al. "Flexible categorization in perceptual decision making". en. In: *Nature Communications* 12.1 (Feb. 2021), p. 1283. ISSN: 2041-1723. DOI: 10.1038/s41467-021-21501-z. URL: <https://www.nature.com/articles/s41467-021-21501-z>.

